



## Original Research article

# A Comparative Study for Adsorption of Alizarin Red S from Aqueous Samples by Magnetic Nanoparticles of $\text{Fe}_3\text{O}_4$ , $\text{CoFe}_2\text{O}_4$ and Ionic Liquid-Modified $\text{Fe}_3\text{O}_4$

Sedigheh Kamran\* , Neda Amiri Shiri

Department of Chemistry, Payame Noor University, PO Box 19395-3697 Tehran, Iran

### ARTICLE INFORMATION

Received: 16 October 2017

Received in revised: 04 Desember 2017

Accepted: 29 December 2017

Available online: 01 January 2018

DOI:

10.22631/chemm.2017.101267.1015

### KEYWORDS

Adsorption

Alizarin Red S

Ionic liquid

Magnetic nanoparticle

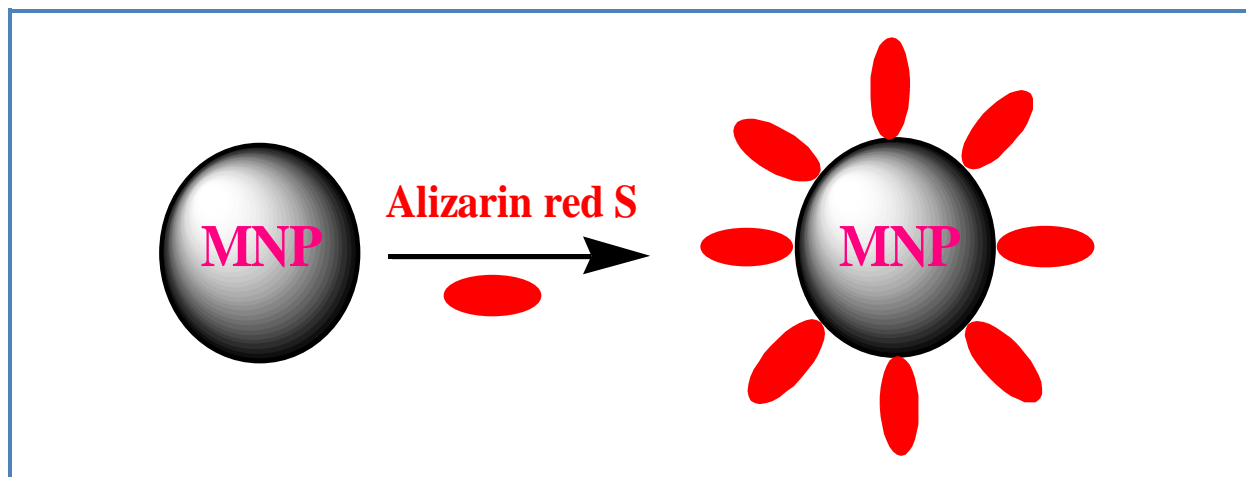
### ABSTRACT

The  $\text{CoFe}_2\text{O}_4$  and  $\text{Fe}_3\text{O}_4$  nanoparticles, and ionic liquid-modified  $\text{Fe}_3\text{O}_4$  with 1-octyl-3-methylimidazolium bromide, (IL- $\text{Fe}_3\text{O}_4$ ), have been prepared and their characteristics for adsorption of alizarin red S dye (ARS) were studied. The mean size and the surface morphology of the nanoparticles were characterized by TEM, XRD and FTIR techniques. Adsorption of the ARS was performed under different experimental conditions in the batch system. The isotherm evaluations showed that the Langmuir model performed better fits with the equilibrium data. The maximum adsorption capacities were 140.8, 192.3, and 256.4 mg of ARS per gram  $\text{Fe}_3\text{O}_4$ ,  $\text{CoFe}_2\text{O}_4$ , and IL- $\text{Fe}_3\text{O}_4$  nanoparticles, respectively. The applicability of two kinetic models including pseudo-first order and pseudo-second order models were estimated as the basis of comparative analysis of the corresponding rate parameters, equilibrium adsorption capacity and correlation coefficients. The adsorption processes for the  $\text{Fe}_3\text{O}_4$  and IL- $\text{Fe}_3\text{O}_4$  nanoparticles as adsorbents were endothermic. Nevertheless the adsorption of ARS onto  $\text{CoFe}_2\text{O}_4$  nanoparticles was exothermic. The dye was desorbed by an alkaline solution at pH 9.0 from  $\text{Fe}_3\text{O}_4$  and by an acidic solution at pH 3.0 from both IL- $\text{Fe}_3\text{O}_4$  and  $\text{CoFe}_2\text{O}_4$  nanoparticles. The recovered nanoparticles were successfully reused for more removal of the dye.

\*Corresponding author: Email address: kamran\_ss5@yahoo.com

Department of Chemistry, Payame Noor University, PO Box 19395-3697 Tehran, Iran

## Graphical Abstract



## Introduction

Different kinds of synthetic dye may be found in the wastewaters formed in textile, leather, paper, and printing industries. Many toxic dyes are stable to photo-degradation, biodegradation, and oxidizing agents. Dyes have some harmful effects on the aquatic life. Dye removal from the wastewaters has attracted a great deal of attention from the researchers over the last few years. This is not only because of the potential toxicity, but also due to visibility problems. Further, a few dyes or their metabolites are either toxic or mutagenic and carcinogenic. In addition, residual dyes in wastewater absorb sunlight, leading to a decrease in the efficiency of the photosynthesis in the aquatic plants [1,2]. The pollution of water owing to color effluents originating from various industrial activities is currently a global environmental problem [3,4]. Therefore, it is necessary to find effective methods for wastewater treatment to remove dyes from the effluents. The methods used to remove the organic dyes and pigments from the wastewaters are classified into three main categories: (i) physical methods (adsorption, filtration, and flotation) [5-7], (ii) chemical methods (oxidation, reduction, and electrochemical) [8,9] and (iii) biological methods (aerobic and anaerobic degradation) [10,11].

The conventional treatment methods for dye effluents such as, oxidation, coagulation, flocculation, photochemical destruction, ion exchange, and membrane filtration are complicated and costly. These methods require additional chemicals or produce toxic products. In fact, the adsorption method has been widely used for dye removal [12].

Adsorption has evolved into one of the most effective physical processes for decolorization of the wastewaters since it can produce high-quality and is economically feasible [13]. The most typically

used adsorbent for the color removal is activated carbon [14], due to its functionality for efficaciously adsorbing a wide range of materials [15]. However, its high cost and difficulty in its regeneration restrict its utilization. Thus, many researchers have focused on investigating the capabilities of nanoparticles. The economic and easily available adsorbent would certainly make an adsorption-based process a viable alternative for the treatment of wastewater containing pollutants. Selection of an appropriate adsorbent is one of the key issues to achieve the maximum removal of a pollutant because the process remarkably depends upon the adsorbent and adsorbate characteristics. Magnetic nanoparticles as an efficient adsorbent with large specific surface area and small diffusion resistance have been recognized [16]. The use of synthetic iron oxide is much more economic than the commercial highly efficient activated carbon, with a 30:1 relative ratio depending on the particular kind of activated carbon [17]. Moreover, the magnetic separation provides a suitable route for online separation. Several articles have been published on the application of various nanoparticles for the treatment and remediation of pollutants in the environment. Some even focusing specifically on dye removal [18, 19] for example, magnetic cellulose/Fe<sub>3</sub>O<sub>4</sub>/activated carbon composite were used for removal of Congo red [20]. Preferential and enhanced adsorption of different dyes was studied on iron oxide nanoparticles [21].

In this work a comparative study was conducted on the adsorption of alizarin red S onto Fe<sub>3</sub>O<sub>4</sub>, CoFe<sub>2</sub>O<sub>4</sub> and, IL-Fe<sub>3</sub>O<sub>4</sub> nanoparticles as adsorbents. The ionic liquid used for this study was 1-octyl-3-methylimidazolium bromide, [C<sub>8</sub>MIM][Br], and the prepared nanoparticles were characterized by transmission electron microscopy (TEM), X-ray diffraction (XRD), and Fourier transform infrared (FTIR) spectroscopy. Adsorption isotherms, kinetic of adsorption and thermodynamic parameters were also characterized and reported.

## Experimental

### Chemicals and reagents

All the chemicals were of analytical grades. Alizarin red S (ARS), sodium hydroxide solution, hydrochloric acid (37 %w/w), acetone, FeCl<sub>3</sub>.6H<sub>2</sub>O (96 %w/w), FeSO<sub>4</sub>.7H<sub>2</sub>O (99.9 %w/w), CoCl<sub>2</sub>, 1-bromooctane, and 1-methylimidazolium were purchased from Merck (Merck, Darmstadt, Germany). For treatment experiments, the dye solution with the concentration range of 10–200 mg L<sup>-1</sup> was prepared through dilution of the stock solution (1000 mg L<sup>-1</sup>) with distilled water. The pH was adjusted by using HCl and NaOH solutions (0.01–1.0 molL<sup>-1</sup>). The ionic liquid, 1-Octyl-3-methylimidazolium bromide, and [C<sub>8</sub>MIM][Br], were prepared in accordance with the procedures reported on the literature [22].

### **Apparatus**

A UV-visible (Shimadzu spectrophotometer Model 1601) equipped with a 1-cm quartz cell was used for recording the visible spectra and absorbance measurements. The XRD measurements were performed using a Bruker D8 AdvanceXRD. The FTIR spectra were recorded on a Shimadzu FTIR 8000 spectrometer. A transmission electron microscope (Philips CM 10 TEM) was used for recording the TEM images. A Metrohm 780 pH meter was used for monitoring the pH values. A waterultrasonicator (Model CD-7810, China) was used to disperse the nanoparticles in solution and a supermagnet Nd-Fe-B(1.4 T, 10×5×2 cm) was used. All the measurements were performed at ambient temperature.

### **Fabrication of the modified Fe<sub>3</sub>O<sub>4</sub> nanoparticles with ionic liquid**

The Fe<sub>3</sub>O<sub>4</sub> nanoparticles were synthesized by mixing ferrous sulfate and ferric chloride in sodium hydroxide solution with constant stirring as advocated. To achieve maximum yield for magnetic nanoparticles during the co-precipitation process, the ideal molar ratio of Fe<sup>2+</sup>/Fe<sup>3+</sup> was about 0.5. The precipitates have been heated at 60 °C for 30 min and had been sonicated for 16 min, then washed for three times with 50 mL of distilled water.

Modification of the Fe<sub>3</sub>O<sub>4</sub> nanoparticles was carried out using [C<sub>8</sub>MIM][Br] under vigorous magnetic stirring for 30 min at 60 °C. The modified iron oxide nanoparticles (IL-Fe<sub>3</sub>O<sub>4</sub>) were collected by applying a magnetic field with an intensity of 1.4 T. The nanoparticles washed three times with 50 mL of distilled water. Nanoparticles were dispersed in the distilled water by using the ultrasonicator for 10 min at room temperature and then were magnetically separated [23].

### **Fabrication of CoFe<sub>2</sub>O<sub>4</sub> nanoparticles**

The cobalt ferrite nanoparticles were synthesized by a co-precipitation technique reported on the literature [24]. An aliquot of 80 mL of an aqueous solution containing 0.11 M Fe<sup>+3</sup> and 0.055 M Co<sup>+2</sup> was continuously added into a reaction vessel containing 150 mL of boiling (90 °C) 0.725 M NaOH under continuous mechanical stirring at 500 rpm. A contact time of 2 h was performed for dehydration and atomic rearrangement and conversion of the intermediate hydroxide phase of the spinel structure. The produced CoFe<sub>2</sub>O<sub>4</sub> nanoparticles were rinsed three times, each time with 50 mL distilled water, and then were magnetically separated.

### **Adsorption experiments**

Aliquots of 20 mL of 10–100 mg L<sup>-1</sup> dye solutions in the pH range of 3.0–10.0 were prepared and transferred into individual beakers. A known amount of nanoparticles in the range of 5.0–35.0 mg was added to each solution, and the suspension was immediately stirred with a magnetic stirrer for

a predefined period of time (5-20 min). After mixing, the nanoparticles were magnetically separated, and the mother liquor was spectrophotometrically analyzed at 520 nm for the residual dye. The percent adsorption of dye, i.e. the dye-removal efficiency of nanoparticles, was determined by using the following equation:

$$\text{Dye removal efficiency (\%)} = \frac{(C_0 - C_f)}{C_0} \times 100 \quad (1)$$

Where  $C_0$  and  $C_f$  represent the dye concentrations ( $\text{mg L}^{-1}$ ) before and after adsorption, respectively.

To observe the effects of temperature, adsorption studies were carried in the temperature range of 15 to 65 °C. To study the adsorption kinetics of the dye, the nanoparticles (20 mg) were incubated with 20ml of a solution (at a specific pH) containing 20  $\text{mg L}^{-1}$  ARS. The suspension was immediately stirred for a selected period of time. Adsorption kinetic data were obtained by measuring the concentration of dye in the solution at different times after removing the magnetic nanoparticles.

## Results and discussion

### Characterization of $\text{Fe}_3\text{O}_4$ , IL- $\text{Fe}_3\text{O}_4$ and $\text{CoFe}_2\text{O}_4$

Almost all the peak positions and relative intensities observed in the XRD pattern of IL- $\text{Fe}_3\text{O}_4$  nanoparticles (Figure 1-B) are consistent in the XRD pattern of the standard  $\text{Fe}_3\text{O}_4$  (Figure 1-A). Although the magnetic nanoparticle surfaces in IL- $\text{Fe}_3\text{O}_4$  were coated with ionic liquid, analysis of XRD patterns of both  $\text{Fe}_3\text{O}_4$  and IL- $\text{Fe}_3\text{O}_4$  indicated distinguishable peaks for magnetite crystal meaning that these particles have phase stability [25].

The FTIR spectra of both  $\text{Fe}_3\text{O}_4$  and IL- $\text{Fe}_3\text{O}_4$  are shown in Figure 2. In the case of  $\text{Fe}_3\text{O}_4$ , the broad absorption band at  $3440 \text{ cm}^{-1}$  indicates the presence of surface hydroxyl groups (O-H stretching) and the bands at low wave numbers ( $\leq 700 \text{ cm}^{-1}$ ) are related to vibrations of the Fe-O bonds in iron oxide. The presence of magnetite nanoparticles can be established via the advent of two strong absorption bands around  $632$  and  $585 \text{ cm}^{-1}$ . The Fe-O bond peak of the bulk magnetite is observed at  $576 \text{ cm}^{-1}$ . In the FTIR spectrum of IL- $\text{Fe}_3\text{O}_4$ , the significant absorption band at  $2923.9 \text{ cm}^{-1}$  is due to the C-H stretching. The absorption band indicating the C-N stretching is observed at  $1447.5 \text{ cm}^{-1}$ . The absorption band at  $1604 \text{ cm}^{-1}$  is related to the hetroaromatic C-H bond stretching.

The TEM image of  $\text{Fe}_3\text{O}_4$  nanoparticles indicated that the average diameter of  $\text{Fe}_3\text{O}_4$  nanoparticles was about  $\sim 10 \text{ nm}$  and that of  $\text{CoFe}_2\text{O}_4$ , was  $\sim 12 \text{ nm}$ . However, the TEM image of IL- $\text{Fe}_3\text{O}_4$  ( $\sim 13 \text{ nm}$ ) indicated that this nanoparticles had a few larger particle diameter than  $\text{Fe}_3\text{O}_4$

revealing that ionic liquid caused agglomeration of  $\text{Fe}_3\text{O}_4$  nanoparticles. This was expected as ionic liquid could reduce the surface charges of nanoparticles [26, 27].

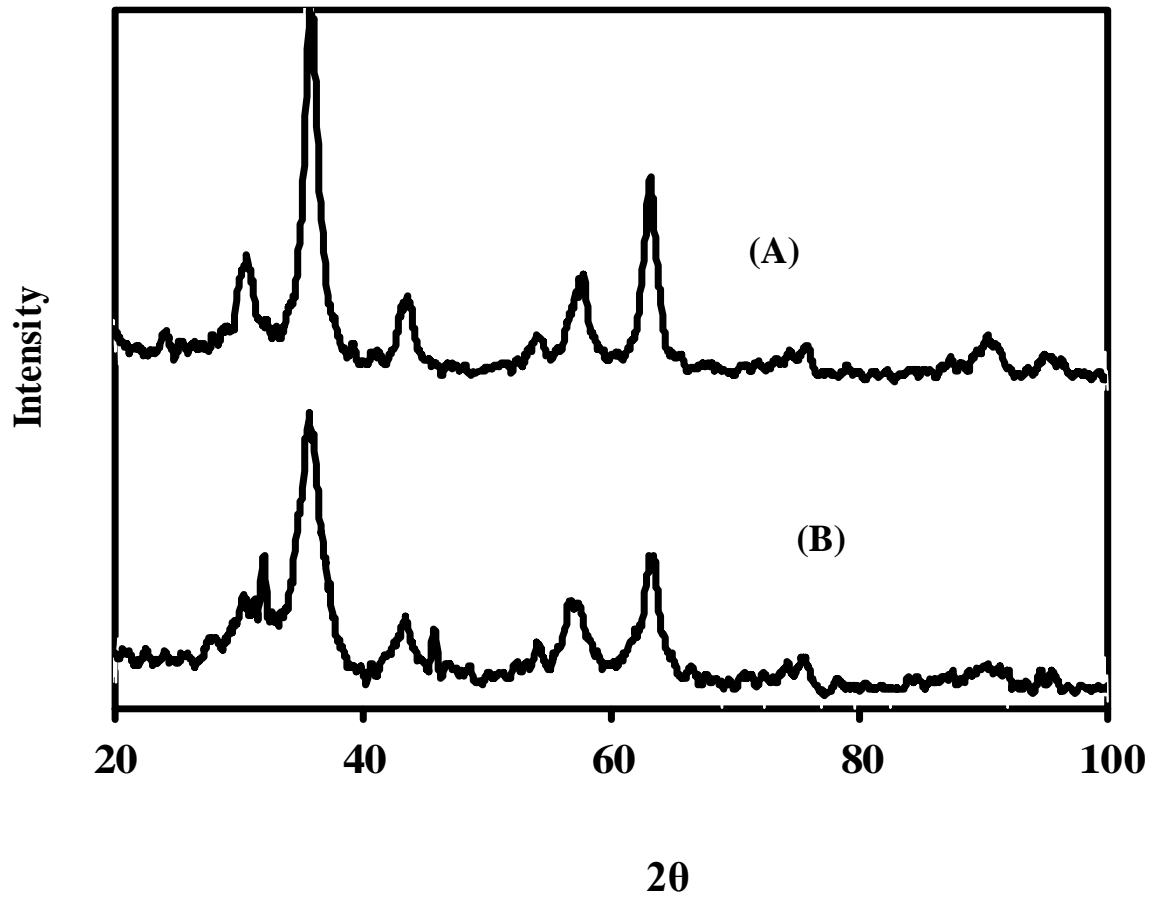


**Figure 1.** XRD pattern of  $\text{Fe}_3\text{O}_4$ , A; and  $\text{IL-Fe}_3\text{O}_4$ , B.

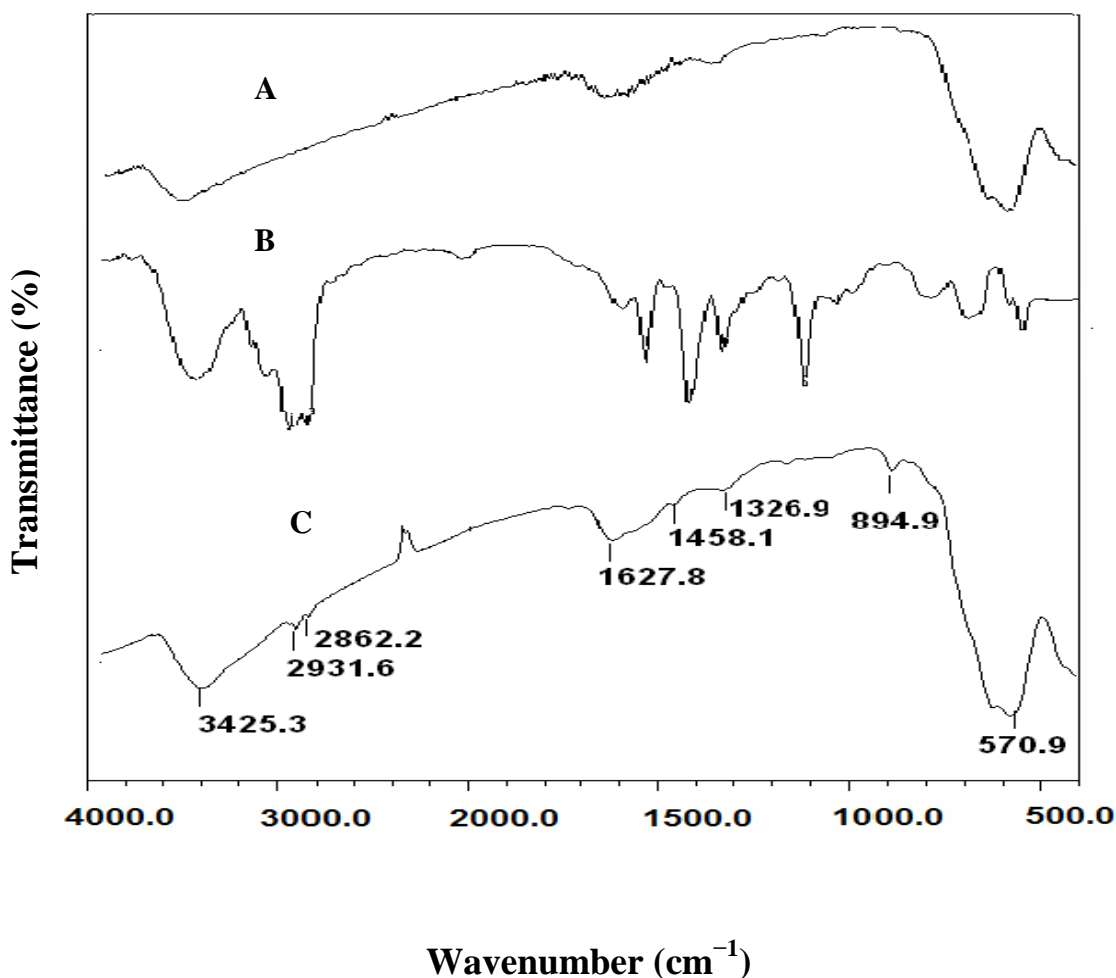


Figure 2. FTIR spectra of  $\text{Fe}_3\text{O}_4$ , A; and IL- $\text{Fe}_3\text{O}_4$ , B.

### Effect of solution pH

Solution pH is an important parameter affecting the adsorption of the dye molecules. The solution pH could affect both aqueous chemistry and surface binding sites of the adsorbent. The influence of the initial pH on the adsorption of the ARS onto  $\text{Fe}_3\text{O}_4$ ,  $\text{CoFe}_2\text{O}_4$ , and IL- $\text{Fe}_3\text{O}_4$  surfaces were assessed at different pH values, ranging from 3.0 to 9.0. The initial concentrations of dye and adsorbents amounts were set at  $20 \text{ mg L}^{-1}$ ,  $5.0 \text{ mg}$ , respectively. Each solution was stirred for a period of 4 min while the experiments were performed in batch technique. The results are depicted in Figure 3.

Figure 3 demonstrates that the initial pH of the solution significantly affects the adsorption of ARS onto the  $\text{CoFe}_2\text{O}_4$  and IL- $\text{Fe}_3\text{O}_4$  nanoparticles. The amount of negatively-charged nanoparticles were

expected to be increased by increasing pH. Therefore, in the pH values lower than  $\sim 3.0$  for both  $\text{CoFe}_2\text{O}_4$  and  $\text{IL-Fe}_3\text{O}_4$  nanoparticles, the percent removal of ARS was firstly increased as long as the dye molecule was present in their positive or neutral forms. At the low pH, the nanoparticles tend to dissolve as reported [28] which was also observed in this study.

For  $\text{CoFe}_2\text{O}_4$  and  $\text{IL-Fe}_3\text{O}_4$  nanoparticles, the anionic form of ARS predominates at pH more than 3.0 and an electrostatic repulsion is developed between both negatively-charged nanoparticles and anionic form of ARS. The result of this experiment is shown in Figure 3. The figure shows a decrease in percent removal of the dye as pH increases to values more than 3.0. Generally, the higher adsorption of dye at lower pH values could be due to the electrostatic attractions between negatively-charged dye anion and the positively-charged nanoparticles, whereas at higher pH values the abundance of  $\text{OH}^-$  is expected to prevent the adsorption of the anionic dye molecules [29]. Figure 3 demonstrates that the adsorption of ARS onto  $\text{Fe}_3\text{O}_4$  nanoparticles is independent of pH. This observation may indicate that dye adsorption not only is influenced by the molecular structure of the ARS, but also by surface specification of the adsorbent.

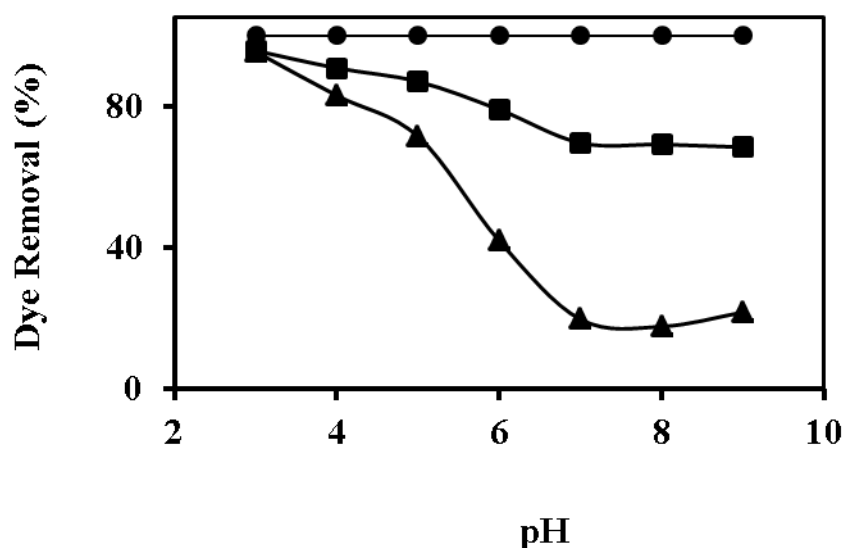


**Figure 3.** Effect of initial pH of dye solution on adsorption of ARS onto  $\text{Fe}_3\text{O}_4$  (●),  $\text{IL-Fe}_3\text{O}_4$  (▲), and  $\text{CoFe}_2\text{O}_4$  (■). Experimental conditions: nanoparticle amount of 20.0, 5.0 and 5.0 mg, respectively, initial dye concentration of  $20 \text{ mg L}^{-1}$ , stirring time of 20 min.

#### Effect of solution temperature

The Gibbs free energy,  $\Delta G^0$  ( $\text{kJ mol}^{-1}$ ), enthalpy,  $\Delta H^0$  ( $\text{kJ mol}^{-1}$ ) and entropy,  $\Delta S^0$  ( $\text{J mol}^{-1}\text{K}^{-1}$ ) of the adsorption processes were calculated using the Van't Hoff thermodynamic equations:



$$\Delta G^0 = -RT \ln K_c \quad (2)$$

$$\ln K_c = -\frac{\Delta H^0}{RT} + \frac{\Delta S^0}{R} \quad (3)$$

where T is the temperature in K and R is the universal gas constant (8.314 J mol<sup>-1</sup> K<sup>-1</sup>). The effect of temperature on the adsorptions of ARS by Fe<sub>3</sub>O<sub>4</sub>, IL-Fe<sub>3</sub>O<sub>4</sub>, and CoFe<sub>2</sub>O<sub>4</sub> nanoparticles are shown in Figure 4A at the temperature ranging from 288 to 338 K. The adsorption efficiency of the Fe<sub>3</sub>O<sub>4</sub> and IL-Fe<sub>3</sub>O<sub>4</sub> for adsorption of ARS, in turn, was about 76% and 83% at 288 K were increased to 96% and 98% at 388 K, respectively. This refers to the endothermic nature of the adsorption process. However, the dye adsorption efficiency of CoFe<sub>2</sub>O<sub>4</sub> was about 98% at 288 K which decreased to 58% at 388 K indicating to the presence of an exothermic dye adsorption process. The plot of lnK<sub>c</sub> (or lnq<sub>e</sub>/C<sub>e</sub>) versus 1/T is indicated in the inset of Figure 4B. From the slope and intercept, the changes of the enthalpy ( $\Delta H$ ) and entropy ( $\Delta S$ ) at 288-388 K could be determined. Table 1 shows thermodynamic parameters of adsorption for adsorption of ARS onto Fe<sub>3</sub>O<sub>4</sub>, CoFe<sub>2</sub>O<sub>4</sub>, and IL-Fe<sub>3</sub>O<sub>4</sub> nanoparticles. The free energy of the adsorption processes at all temperatures was negative indicating the feasibility of the process and the spontaneous nature of the adsorption processes.

**Table 1.** Thermodynamic parameters of dye-adsorption processes onto IL-Fe<sub>3</sub>O<sub>4</sub>, CoFe<sub>2</sub>O<sub>4</sub>.

Adsorbent	$\Delta H_0^r$ (kJmol <sup>-1</sup> )	$\Delta S_0^r$ (kJmol <sup>-1</sup> )	$\Delta G_0^r$ (kJmol <sup>-1</sup> )					
			288K	298K	308K	318K	328K	338K
Fe <sub>3</sub> O <sub>4</sub>	15.98	65.51	-2.88	-3.53	-4.19	-4.84	-5.5	-6.15
CoFe <sub>2</sub> O <sub>4</sub>	-22.09	44.75	-34.99	-35.43	-35.88	-36.33	-36.78	-37.22
IL-Fe <sub>3</sub> O <sub>4</sub>	33.613	124.46	-2.23	-3.47	-4.72	-5.96	-7.20	-8.45

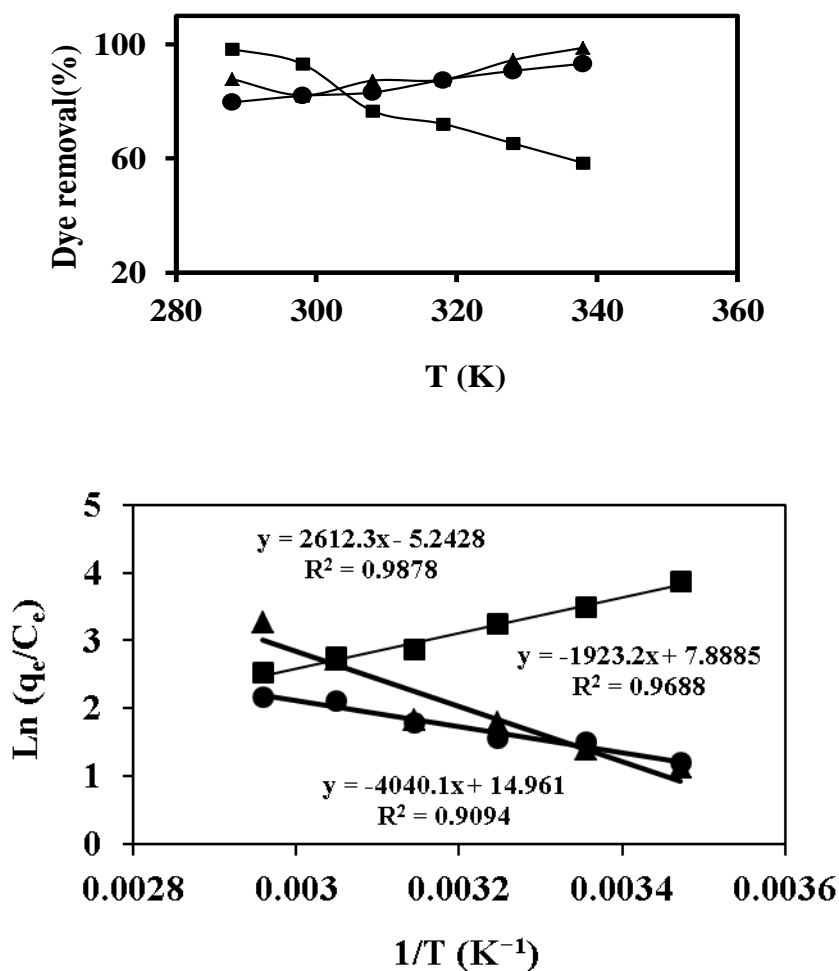


**Figure 4.** (A) Effect of temperature on adsorption of ARS onto Fe<sub>3</sub>O<sub>4</sub>(●); CoFe<sub>2</sub>O<sub>4</sub> (■) and IL-Fe<sub>3</sub>O<sub>4</sub> (▲). 5(B), The plots of ln(q<sub>e</sub>/C<sub>e</sub>) against 1/T for adsorption of ARS onto Fe<sub>3</sub>O<sub>4</sub> (●); CoFe<sub>2</sub>O<sub>4</sub> (■) and IL-Fe<sub>3</sub>O<sub>4</sub> (▲). Experimental conditions: nanoparticle amount of 20.0, 5.0 and 5.0 mg, respectively, initial dye concentration of 20 mg L<sup>-1</sup>, solution pH of 3.0 and stirring time of 20 min.

The negative  $\Delta G$  indicated that the adsorption was proportional to the temperature. The positive value of  $\Delta H$  indicated that adsorption processes for dye onto Fe<sub>3</sub>O<sub>4</sub> and IL-Fe<sub>3</sub>O<sub>4</sub> were endothermic. The negative value of  $\Delta H$  indicated that dye adsorption onto CoFe<sub>2</sub>O<sub>4</sub> was exothermic. The positive value of the  $\Delta S$  indicated that the dye molecules adsorbed on the surface of the nanoparticles. This could be explained by the fact that the dye molecules are hydrated in the solution through hydrogen bonding, therefore the dehydration of dye molecules and loss of the water molecules increased the

degree of disorder in the system. The adsorption affinity of the dye molecules on the surface of three nanoparticles gives some order to the system. Therefore, dehydration entropy predominates over adsorption affinity entropy and consequently the entropy of adsorption is positive. [30].

### Adsorption isotherm modeling

The adsorption isotherm of a specific adsorbent represents its adsorptive characteristics, which are very important for designing the adsorption processes. Several isotherm models for evaluating the equilibrium adsorption have discussed in literatures [31]. Experiments for the estimation of the individual adsorption isotherms of ARS onto IL-Fe<sub>3</sub>O<sub>4</sub> and Fe<sub>3</sub>O<sub>4</sub> and CoFe<sub>2</sub>O<sub>4</sub> surfaces were performed by adding various amounts of IL-Fe<sub>3</sub>O<sub>4</sub>, Fe<sub>3</sub>O<sub>4</sub> and CoFe<sub>2</sub>O<sub>4</sub> in the range of 5-20 mg, to a series of beakers containing 20 mL of 10-100 mg L<sup>-1</sup> of the dye solution at pH 3.0-9.0. The solutions were stirred for 20 min at 25 °C to attain the equilibrium condition. The aqueous solutions were analyzed for the residual dye after applying the magnetic field for settlement of the nanoparticles. The amount of the dye adsorbed onto IL-Fe<sub>3</sub>O<sub>4</sub>, Fe<sub>3</sub>O<sub>4</sub> and CoFe<sub>2</sub>O<sub>4</sub> nanoparticles were calculated based on the following equation:

$$q_e = \frac{V(C_0 - C_e)}{m} \quad (4)$$

Where  $q_e$  (in mg g<sup>-1</sup>) is the adsorption capacity (mg dye adsorbed onto a gram amount of nanoparticles),  $V$  is the volume of the dye solution (in liter),  $C_0$  and  $C_e$  are the initial and equilibrium dye concentrations (in mg L<sup>-1</sup>), respectively; and  $m$  is the mass (gram) of the dry IL-Fe<sub>3</sub>O<sub>4</sub>, Fe<sub>3</sub>O<sub>4</sub> and CoFe<sub>2</sub>O<sub>4</sub> added.

The equilibrium adsorption of the ARS on Fe<sub>3</sub>O<sub>4</sub>, CoFe<sub>2</sub>O<sub>4</sub> and IL-Fe<sub>3</sub>O<sub>4</sub> surfaces was analyzed using Langmuir and Freundlich models. Model fits to equilibrium adsorption results of dye were assessed based on the values of the determination coefficient ( $R^2$ ) of the linear regression plot. The experimental data were fit with both models; the resulting plots are shown in Figure 5. Table 2 summarizes the models constants and the determination coefficients. As shown in Table 2 the  $R^2$  of the Langmuir isotherm was greater than that of the Freundlich isotherm for dye adsorption onto three investigated nanoparticles. This indicates that the adsorption of ARS onto Fe<sub>3</sub>O<sub>4</sub>, CoFe<sub>2</sub>O<sub>4</sub> and IL-Fe<sub>3</sub>O<sub>4</sub> nanoparticles is better described by the Langmuir model. This in turn suggests that adsorption occurs as the monolayer dye adsorbs onto the homogenous adsorbents surfaces.

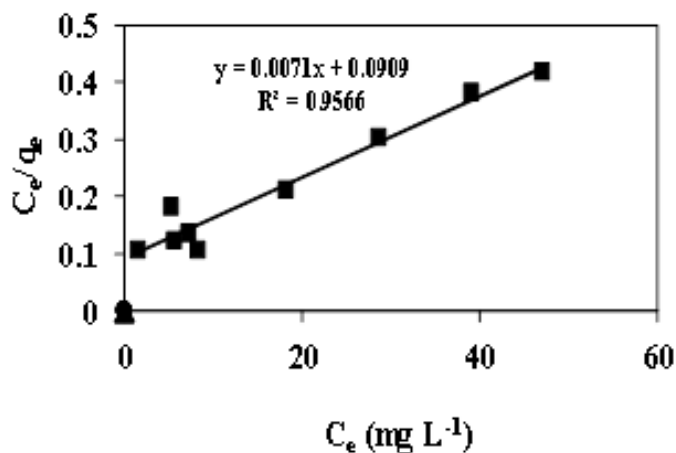


**Figure 5 (A);** Langmuir isotherm plots; **9(B)**, Freundlich isotherm plots for ARS adsorption onto  $\text{Fe}_3\text{O}_4$  (●); and IL- $\text{Fe}_3\text{O}_4$  (▲); and  $\text{CoFe}_2\text{O}_4$  (■) nanoparticles. Experimental conditions:nanoparticle amount of 20.0, 5.0 and 5.0 mg, respectively, stirring time of 20 minutes solution pH of 3.0.

**Table 2.** Adsorption isotherms parameters of ARS onto IL- $\text{Fe}_3\text{O}_4$ , $\text{CoFe}_2\text{O}_4$  and  $\text{Fe}_3\text{O}_4$ .

Adsorbent	Langmuir model			Freundlich model		
	$q_{\max}$	$b$	$R^2$	$K_F$	$n$	$R^2$
$\text{Fe}_3\text{O}_4$	140.8	0.078	0.956	15.1	1.78	0.873
$\text{CoFe}_2\text{O}_4$	192.3	0.197	0.942	54.1	2.99	0.940
IL- $\text{Fe}_3\text{O}_4$	256.4	0.28	0.970	94.9	3.99	0.835

Table 2 shows that the maximum adsorption capacity for ARS is 140.8, 192.3, 256.4 mg dye per gram  $\text{Fe}_3\text{O}_4$ ,  $\text{CoFe}_2\text{O}_4$  and IL- $\text{Fe}_3\text{O}_4$  nanoparticles, respectively. The difference in adsorption capacities of the three nanoparticles for adsorption of ARS may be attributed to active sites on the adsorbents. Adsorption capacity of the IL- $\text{Fe}_3\text{O}_4$  is higher than that of the other samples. The adsorption of ARS on the IL- $\text{Fe}_3\text{O}_4$  nanoparticles is attributed to the surface electrostatic and hydrophobic interactions between the dye and IL- $\text{Fe}_3\text{O}_4$  nanoparticles. Hydrocarbon chain of ionic liquid to the surface of IL- $\text{Fe}_3\text{O}_4$  nanoparticles could be responsible for hydrophobic interaction between the dye and nanoparticle. The adsorption of ARS onto  $\text{Fe}_3\text{O}_4$ ,  $\text{CoFe}_2\text{O}_4$  is due to the interaction between the functional groups of the ARS (OH) and the surface hydroxyl groups of both nanoparticles.

### Adsorption kinetic modeling

Several models describe the adsorption mechanism. The most commonly models used are the pseudo-first-order and pseudo-second-order reaction rate equations [32, 33] developed by [34] which have the following linear forms for boundary conditions of  $q=0$  at  $t=0$  and  $q_t=q_e$  at  $t=t_e$ .

Pseudo-first-order equation: 
$$\log(q_e - q_t) = \log q_e - k_1 t \quad (5)$$

Pseudo-second-order equation: 
$$\frac{t}{q_t} = \frac{1}{k_2 q_e^2} + \frac{t}{q_e} \quad (6)$$

where  $k_1$  and  $k_2$  are the adsorption rate constants,  $q_t$  is adsorption capacity at time  $t$ ,  $q_e$  is adsorption capacity at equilibrium condition. To describe the adsorption behavior and rate, the data obtained from adsorption kinetic experiments were evaluated using pseudo-first and pseudo-second-order reaction rate models. Table 3 provides a summary of the models and constants along with the correlation coefficients for the linear regression plots of three adsorption processes. As shown in Table 3, the theoretical  $q_e$  value estimated from the first order kinetic model gave significantly different value compared to experimental value and was found to be lower. Higher values of  $R^2$  were obtained for pseudo-second-order than for pseudo-first-order adsorption rate models indicating that the adsorption rates of ARS onto  $Fe_3O_4$ ,  $CoFe_2O_4$  and  $IL-Fe_3O_4$  nanoparticles can be more appropriately described using the pseudo-second-order rate.

**Table 3.** Adsorption kinetic parameters of dye-adsorption processes onto  $IL-Fe_3O_4$ ,  $CoFe_2O_4$ ,  $Fe_3O_4$  nanoparticles.

Adsorbent	Pseudo-first-order model			Pseudo-second-order model		
	$k_1$ ( $\text{min}^{-1}$ )	$q_e$ ( $\text{mg g}^{-1}$ )	$R^2$	$k_2$ ( $\text{g mg}^{-1}\text{min}^{-1}$ )	$q_e$ ( $\text{mg g}^{-1}$ )	$R^2$
<b>Fe<sub>3</sub>O<sub>4</sub></b>	0.013	0.011	0.939	165	17.3	1.0
<b>CoFe<sub>2</sub>O<sub>4</sub></b>	0.084	1.045	0.423	0.042	58.8	0.986
<b>IL-Fe<sub>3</sub>O<sub>4</sub></b>	0.073	10.51	0.938	0.029	83.8	0.999

### Desorption and reusability of adsorbents

For potential practical applications, the regeneration and reuse of an adsorbent are important. Possible desorption of ARS was tested by using different solutions such as pure methanol, sodium chloride solution ( $1.0 \text{ mol L}^{-1}$ ), sodium hydroxide solution ( $1.0 \text{ mol L}^{-1}$ ), mixed sodium chloride ( $1.0 \text{ mol L}^{-1}$ )/acetone (with volume ratios of 1:1, 2:1 and 1:2) and solution with different pH 3.0, 9.0. The study revealed that the adsorbed ARS could be completely desorbed in the presence of solution with pH 3.0, 9.0. In this study, more than 89%, 85% and 91% of ARS could be desorbed and recovered by 30 mL of solution with different pH 3.0, 9.0, when 0.4 mg dye (20 mL of dye with a

concentration of 20 mg L<sup>-1</sup>) was already adsorbed on Fe<sub>3</sub>O<sub>4</sub>, IL-Fe<sub>3</sub>O<sub>4</sub> and CoFe<sub>2</sub>O<sub>4</sub> nanoparticles. Addition of desorbing solution in multiple steps (3 steps as was obtained) can improve the desorption process as expected.

### Conclusions

The mean size and the surface morphology of Fe<sub>3</sub>O<sub>4</sub>, CoFe<sub>2</sub>O<sub>4</sub> and IL-Fe<sub>3</sub>O<sub>4</sub> nanoparticles were characterized by TEM, XRD, and FTIR techniques. The FTIR analysis demonstrated the attachment of [C<sub>8</sub>MIM][Br] on the surface of Fe<sub>3</sub>O<sub>4</sub> nanoparticles. It was achieved through the interaction between the cationic part of [C<sub>8</sub>MIM][Br] and the surface hydroxyl groups of Fe<sub>3</sub>O<sub>4</sub>. Adsorption studies of ARS were performed under different experimental conditions in batch technique. Experimental results indicated that Fe<sub>3</sub>O<sub>4</sub>, CoFe<sub>2</sub>O<sub>4</sub>, and IL-Fe<sub>3</sub>O<sub>4</sub> nanoparticles removed more than 98% of dye under the optimum condition. The comparative study was shown that the IL-Fe<sub>3</sub>O<sub>4</sub> nanoparticles were quite efficient as adsorbents for the fast removal of dye from the aqueous solutions. Short contact time, high adsorption capacity, stability and reusability are advantages of IL-Fe<sub>3</sub>O<sub>4</sub> and CoFe<sub>2</sub>O<sub>4</sub> nanoparticles. The isotherm evaluations revealed that the Langmuir model attained better fits with the equilibrium data. The maximum adsorption capacities were 140.8, 192.3 and 256.4 mg of alizarin red S per gram of Fe<sub>3</sub>O<sub>4</sub>, CoFe<sub>2</sub>O<sub>4</sub> and IL-Fe<sub>3</sub>O<sub>4</sub> nanoparticles, respectively. The changes of enthalpy ( $\Delta H$ ) were determined to be 15.98, -22.09 and 33.61 kJ mol<sup>-1</sup> for Fe<sub>3</sub>O<sub>4</sub>, CoFe<sub>2</sub>O<sub>4</sub> and IL-Fe<sub>3</sub>O<sub>4</sub>, in the same order.

### Acknowledgments

The authors would like to acknowledge the Payame Noor University for its support. We also appreciate Prof. G. Absalan from the department of chemistry, Shiraz University. Department of physics, engineering department and veterinary college at Shiraz University are also acknowledged for their technical assistance.

### References

- [1] Forgacs E., Cserhati T., Oros G. *Environ. Int.*, 2004, **30**:953
- [2] Oladipo A.A, Gazi M., Yilmaz E. *Chem. Eng. Res. Des.*, 2015, **104**:264
- [3] Panda N., Sahoo H., Mohapatra S. *J. Hazard. Mater.*, 2011, **185**:359
- [4] Mittal A., Gupta V.K. *Toxicol. Environ. Chem.*, 2010, **92**:1813
- [5] Afkhami A., Moosavi R. *J. Hazard. Mater.*, 2010, **174**:398
- [6] Zheng Y., Yao G., Cheng Q., Yu S., Liu M., Gao C. *Desalination*, 2013, **328**:42
- [7] Wang S., Li H., Xu L. *J. Colloid. Interf. Sci.*, 2006, **295**:71
- [8] Gutierrez M.C., Pepio M., Crespi M. *Color Technol.*, 2002, **118**:1

- [9] Gupta V.M , Jain R., Varshney S. *J. Colloid Interf. Sci.*, 2007, **312**:292
- [10] Quan X., Zhang X., Xu H. *Water Res.*, 2015, **78**:74
- [11] Kapdan I.K., Ozturk R. *J. Hazard . Mater.*, 2005, **123**:217
- [12] Wang L., Li J. *Indust. Crops. Prod.*, 2013, **42**:153
- [13] Ozcan A., Ozcan A.S. *J. Hazard. Mater.*, 2005, **125**:252
- [14] Ghaedi M., Najibi A., Hossainian H., Shokrollahi A. and Soylak M. *Toxicol. Environ. Chem.*, 2012, **94**:40
- [15] Oliveira L.C.A., Rios R.V.R.A., Fabris J.D., Garg V., Sapag K., Lago R.M. *Carbon*, 2002, **40**:2177
- [16] Ghaedi M., Hassanzadeh A., NasiriKokhdan S. *J. Chem. Eng.*, 2011, **56**:2511
- [17] Pirillo S., Ferreira M.L., Rueda E.H. *Ind. Eng. Chem. Res.*, 2007, **46**:8255
- [18] Hu Z.G., Zhang J., Chan W.L., Szeto Y.S. *Polymer*, 2006, **47**:5838
- [19] Du H.W.L., Xu Z.R., Han X.Y., Xu Y.L., Miao Z.G. *J. Hazard. Mater.*, 2008, **153**:152
- [20] Zhu H.Y., Fu Y.Q., Jiang R., Jiang J.H., Xiao L., Zeng G.M., Zhao S.L., Wang Y. *Chem . Eng. J.*, 2011, **173**:494
- [21] Saha B., Das S., Saikia J., Das G. *J. Phy. Chem.*, 2011, **115**:8024
- [22] Bonhote P., Dias A.P., Papageorgion N., Kalyanasundaran K., Gratzel M. *Inorg. Chem.*, 1996, **35**:1168
- [23] Kamran S., Asadi M., Absalan G. *Anal. Methods.*, 2014, **6**:798
- [24] Chinnasamy C.N., Senoue M., Jeyadevan B., Perales-Perez O., Shinoda K., Tohji K. *Appl. Phys. Lett.*, 2003, **85**:2862
- [25] Kamran S., Asadi M., Absalan G. *Micro. Chim. Acta.*, 2013, **180**:41
- [26] Kamran S., Absalan G. Asadi M. *Amino. Acids.*, 2015, **47**:2483
- [27] Ghaemi M., Absalan G., Sheikhian L. *J. Iran. Chem. Soc.*, 2014, **11**:1759
- [28] Zargar B., Parham H., Hatamie A. *Talanta*, 2009, **77**:1328
- [29] Hameed B.H., Ahmad A.A., Aziz N. *Chem. Eng. J.*, 2007, **133**:195
- [30] Absalan G., Asadi M., Kamran S., Sheikhian L., Goltz D. *J. Hazard. Mater.*, 2011, **192**:476
- [31] Limousin G., Gaudet P., Charlet L., Szenknect S., Barthés V., Krimissa M. *Appl. Geochem.*, 2007, **22**:249
- [32] Santos S.C.R., Vilar V.J.P., Boaventura R.A.R. *J. Hazard. Mater.*, 2008, **153**:999
- [33] Ho Y.S., McKay G. *Process. Biochem.*, 1999, **34**:451
- [34] Ho Y.S., McKay G., Wase D.A.J., Foster C.F. *Adsorption Sci. Technol.*, 2000, **18**:639

**How to cite this manuscript:** Sedigheh Kamran\*, Neda Amiri Shiri. A Comparative Study for Adsorption of Alizarin Red S from Aqueous Samples by Magnetic Nanoparticles of  $\text{Fe}_3\text{O}_4$ ,  $\text{CoFe}_2\text{O}_4$  and Ionic Liquid-Modified  $\text{Fe}_3\text{O}_4$ . *Chemical Methodologies* 2(1), 2018, 23-38. DOI: [10.22631/chemm.2017.101267.1015](https://doi.org/10.22631/chemm.2017.101267.1015).